2016 IEEE Innovative Smart Grid Technologies - Asia (ISGT-Asia)
Melbourne, Australia, Nov 28 - Dec 1, 2016

LMP Decomposition with Three-Phase DCOPF for Distribution System

Wei Wang
Department of Electrical and Computer Engineering
University of California, Riverside
Riverside, USA
wwang031@ucr.edu

Nanpeng Yu
Department of Electrical and Computer Engineering
University of California, Riverside
Riverside, USA
nyu@ece.ucr.edu

***Abstract*—This paper presents a three-phase iterative direct current optimal power flow (DCOPF) algorithm with fictitious nodal demand. Power losses and realistic distribution system operating constraints such as line flow limits and phase imbalance limits are carefully modeled in the DCOPF formulation. The definition of locational marginal prices (LMPs) is extended to three-phase distribution systems. The three-phase LMP decomposition is derived based on the Lagrangian function. The proposed algorithm is implemented in an IEEE test case and compared with three-phase alternating current optimal power flow (ACOPF) algorithm. The simulation results show that the proposed DCOPF algorithm is effective in coordinating the operations of distributed energy resources (DERs) and managing phase imbalance and thermal overloading. The proposed iterative three-phase DCOPF algorithm provides not only a computationally efficient solution but also a good approximation to the ACOPF solution.**

***Index Terms*—demand response, distribution system operator, locational marginal price, three-phase DCOPF.**

NOMENCLATURE

B_{ik}^{pm}, G_{ik}^{pm}	Susceptance and conductance between node *i* with phase *p* and node *k* with phase *m*.
$Cd\,(n,m)_j$	Demand bid price of the *j*-th segment of price sensitive demand bid curve at node *n* with phase *m*.
$Cg\,(1)_i$	Supply offer price of the *i*-th segment of supply offer curve at the reference bus.
$Cg\,(n,m)_i$	Supply offer price of the *i*-th segment of supply offer curve at node *n* with phase *m*.
$d\,(n,m)_j$	Demand bid quantity of the *j*-th segment of price sensitive demand bid curve at node *n* with phase *m*.
$(DF_s^t)^p$	Phase *p*'s delivery factor at node *s* with phase *t*.
FD_i^g	Real power of fixed demand at node *i* with phase g.
FP, FQ	Set of real and reactive power branch flows.
FP_b^p, FQ_b^p	Real and reactive power flow on branch b with phase *p*.
$g\,(n,m)_i$	Supply offer quantity of the *i*-th segment of supply offer curve at node *n* with phase *m*.
$GSFP_{ik\_q}^{p\_g}$	Generation shift factor for real power flow of the branch which connects node *i* and *k* with phase p when power injection is at node q with phase g.
$GSFQ_{ik\_q}^{p\_g}$	Generation shift factor for reactive power flow of the branch which connects node *i* and *k* with phase *p* when power injection is at node *q* with phase g.
J_1	Total number of segments of demand bid curve at the reference bus.
J_n^m, K_n^m	Total number of segments of supply offer curve and demand bid curve at node *n* with phase *m*.
I_{ik}, V_{ik}	Current and voltage across the branch connecting node *i* and *k*.
$(LF_s^t)^p$	Phase *p*'s loss factor at node *s* with phase *t*.
N	Total number of nodes including the swing bus.
PD_n^m	Real power of total demand at node *n* with phase *m*.
PG_n^m	Real power of generation at node *n* with phase *m*.
P_i^p, Q_i^p	Net injection of real and reactive power at node *i* with phase *p*.
P_{ik}^p, Q_{ik}^p	Real and reactive power flowing from node *i* to node *k* with phase *m*.
P_{loss}^p	Total real power losses at phase *p*.
$PLimit_{ik}^p$	Real power flow limit between node *i* and *k* with phase *p*.
R_{ik}^{pg}, X_{ik}^{pg}	Resistance and reactance of the phase impedance matrix relating node *i* with phase *p* and node *k* with phase g.
S_{ik}^p	Complex power flowing from node *i* to node *k* with phase *m*.
$(S_{loss})_{ik}$	Complex power losses of the branches connecting node *i* and *k*.
$SLimit_{ik}^p$	Complex power flow limit between node *i* and *k* with phase *p*.
Z_{ik}	Phase impedance matrix of the line connecting node *i* and *k*.
γ	Power imbalance limit between phases.
$\theta_V{}_{ik}^{pm}$,$\theta_I{}_{ik}^{pg}$	Voltage angle difference and current angle difference between node *i* with phase *p* and node *k* with phase *m*.

978-1-5090-4303-3/16/$31.00 ©2016 IEEE

I. Introduction

Traditionally, the OPF problem is formulated at the transmission system level to find the optimal dispatch levels of generation power plants to meet electricity demand with least cost. The LMP concept not only effectively manages congestion in market operations but also provides guidance to future generation and transmission upgrades. The LMP decomposition method makes cost of congestion transparent. Driven by strict environmental regulations, distributed renewable generation, demand response, and energy storage devices are being deployed in the distribution system at an unprecedented speed. Three-phase OPF problem needs to be effectively solved by distribution system operators in order to efficiently utilize DERs and operate distribution system in a reliable and efficient manner.

Many researchers have studied the problem of DERs coordination and management. In [1], the concept of LMP for distribution system is first proposed in order to manage distribution generation (DG) resources and reduce lines losses. A real-time pricing strategy is used to schedule load with a linear-programming (LP) method in [2]. Researchers in [3] provide a two-stage pricing approach for residential demand response management. In [4], [5], an innovative proactive demand participation scheme is proposed under two-stage pricing framework with demand bid curve forecasting. To mitigate power quality issues of micro-grid, a mixed integer programming (MIP) approach is studied in [6].

However, only a few papers studied the three-phase OPF problem. A quasi-Newton method based approach is developed after transforming the OPF problem with implicit function theorem in [7]. Authors in [8] developed a distributed semidefinite programming solver based on alternating direction method of multipliers (ADMM) for non-convex optimization problem of three-phase alternate current optimal power flow (ACOPF). A comparison of three distributed OPF algorithms including, the auxiliary problem principle (APP), the predictor corrector proximal multiplier method (PCPM), and the alternating direction method (ADM), is conducted in [9]. The main challenge of transforming the original ACOPF problem into a convex optimization problem is the rank constraint. In order to convexify the original ACOPF problem, some recent literatures directly relax the rank constraint [8], [10]–[13]. However, the global optimality is only proved for single-phase tree-networks [14], [15]. Rank reduction techniques can be leveraged to develop heuristic algorithms that solve rank-constrained optimization problems [16]–[18]. However, the convergence of these algorithm cannot be guaranteed.

A regional distribution system typically has thousands of feeders with millions of nodes. It is computationally challenging to solve thousands of convexified large-scale three-phase ACOPF problems in real time. This paper fills the knowledge gap by extending the iterative single-phase DCOPF algorithm [19] to three-phase system with fictitious nodal demand (FND). The proposed iterative three-phase DCOPF algorithm provides not only a computationally efficient solution but also a good approximation to the ACOPF solution. In addition, none of the existing literatures have touched on the subject of LMP decomposition in three-phase distribution system. This paper presents a generalized three-phase LMP decomposition within the DCOPF framework.

The remainder of this paper is organized as follows. Section II formulates the linear model of three-phase DCOPF problem. Section III derives three-phase LMP decomposition from the Lagrangian function. The numerical study results are presented in Section IV. The conclusions are stated in Section V.

II. Three-Phase Iterative DCOPF Formulation

A. Linear Model without Considering Loss

The objective of three-phase DCOPF problem is to maximize total surplus of customers and producers in a distribution system. On the supply side, an equivalent system supply offer curve is created at the point-of-integration to the transmission system. On the demand side, individual buildings and customers express their energy usage preferences by constructing price-sensitive demand bid curves [4]. Node 1, the point-of-integration to the transmission system, is selected as the swing bus of the distribution system. Note that there is only one supply offer curve for all three phases at the distribution substation. The objective function of the DCOPF problem is provided in equation (1). Without considering losses, the real power balance constraints are represented by equation (2). In subsection II.C, these constraints are modified when real power losses are taken into consideration. Equation (3) shows the power flow limit constraints. Generating shift factors used in the equation are derived in subsection II.B. Phase imbalance constraints are represented in equation (4), which have been shown to be effective in mitigating phase imbalance problems in [3].

$$\max_{d} \sum_{n=2}^{N} \sum_{m=1}^{3} \left(\sum_{j=1}^{K_n^m} C_d\left(n,m\right)_j d\left(n,m\right)_j - \sum_{i=1}^{J_n^m} Cg\left(n,m\right)_i g\left(n,m\right)_i \right) - \sum_{i=1}^{J_1} Cg\left(1\right)_i g\left(1\right)_i \quad (1)$$

subject to:

$$\sum_{n=1}^{N} PG_n^m = \sum_{n=1}^{N} PD_n^m, m = 1,2,3 \quad (2)$$

$$|\sum_{q=2}^{N} \sum_{g=1}^{3} GSFP_{ik\_q}^{p\_g} \cdot \left(PG_q^g - PD_q^g\right)| \le PLimit_{ik}^p, \quad \forall i,k \quad and \quad i \ne k \quad (3)$$

$$|\sum_{n=2}^{N} P_n^i - \sum_{n=2}^{N} P_n^j| \le \gamma,\ i,j = 1,2,3\ \ and\ \ i \ne j \quad (4)$$

where

$$PLimit_{ik}^p = \sqrt{(SLimit_{ik}^p)^2 - (\sum_{q=2}^{N} \sum_{g=1}^{3} GSFQ_{ik\_q}^{p\_g} \cdot Q_q^g)^2}$$

B. Derivation of Generation Shift Factors

The relationship between real power injection and voltage angle is derived by differentiating load flow equation with respect to θ_V. We start the derivation from equations (5)-(6) [20]:

$$\frac{\partial P_i^p}{\partial {\theta_V}_k^m} = |V_i^p||V_k^m|[G_{ik}^{pm} sin{\theta_V}_{ik}^{pm} - B_{ik}^{pm} cos{\theta_V}_{ik}^{pm}], \quad p \neq m \text{ or } i \neq k \tag{5}$$

$$\frac{\partial P_i^p}{\partial {\theta_V}_i^p} = -B_{ii}^{pp}(V_i^p)^2 - Q_i^p \tag{6}$$

Under most operational scenarios, the voltage drop and voltage angle bias are small when the distribution network is not heavily loaded or seriously unbalanced. When large voltage drop happens, step-type voltage regulators, load tap changing transformers, and shunt capacitors will be operated to keep customers' voltage within an acceptable range. Thus the following assumptions are made:

$$|V_i^p| \approx 1 \tag{7}$$

$${\theta_V}_{ik}^{pm} \approx \begin{cases} 120^\circ & \text{if } p-m=-1,2 \\ -120^\circ & \text{if } p-m=1,-2 \\ 0^\circ & \text{if } p-m=0 \end{cases} \tag{8}$$

With the above assumptions, equations (5) and (6) can be simplified as:

$$\frac{\partial P_i^p}{\partial {\theta_V}_k^m} = G_{ik}^{pm} sin{\theta_V}_{ik}^{pm} - B_{ik}^{pm} cos{\theta_V}_{ik}^{pm}, \quad p \neq m \text{ or } i \neq k \tag{9}$$

$$\frac{\partial P_i^p}{\partial {\theta_V}_i^p} = -B_{ii}^{pp} - Q_i^p \tag{10}$$

Excluding the swing bus, in condensed form equations (9)-(10) become:

$$\Delta P = [B_P]\Delta\theta_V \tag{11}$$

where $[B_P]$ is a $3(N-1) \times 3(N-1)$ matrix.

The relationship between reactive power injection and voltage magnitude is derived by differentiating load flow equation with respect to V [20]:

$$\frac{\partial Q_i^p}{\partial V_k^m} = |V_i^p|[G_{ik}^{pm} sin{\theta_V}_{ik}^{pm} - B_{ik}^{pm} cos{\theta_V}_{ik}^{pm}], \quad p \neq m \text{ or } i \neq k \tag{12}$$

$$\frac{\partial Q_i^p}{\partial V_i^p} = \sum_{k=1}^{N}\sum_{m=1}^{3} |V_k^m|[G_{ik}^{pm} sin{\theta_V}_{ik}^{pm} - B_{ik}^{pm} cos{\theta_V}_{ik}^{pm}] - |V_i^p| B_{ii}^{pp} cos{\theta_V}_{ii}^{pp} \tag{13}$$

With the same assumption above, equation (12) can be simplified as:

$$\frac{\partial Q_i^p}{\partial V_k^m} = G_{ik}^{pm} sin{\theta_V}_{ik}^{pm} - B_{ik}^{pm} cos{\theta_V}_{ik}^{pm} \quad p \neq m \text{ or } i \neq k \tag{14}$$

As the shunt component is usually very small

$$\sum_{k=1}^{N} B_{ik}^{pm} \approx 0, \quad \sum_{k=1}^{N} G_{ik}^{pm} \approx 0, \quad m = 1,2,3$$

Thus

$$\frac{\partial Q_i^p}{\partial V_i^p} \approx -B_{ii}^{pp} \tag{15}$$

Excluding the swing bus, in condensed form equations (13)-(14) become:

$$\Delta Q = [B_Q]\Delta V \tag{16}$$

where $[B_Q]$ is a $3(N-1) \times 3(N-1)$ matrix.

The complex power flowing from node *i* to *k* with phase *p* is given by (17):

$$S_{ik}^p = V_i^p \sum_{m=1}^{3} [(G_{ik}^{pm} + jB_{ik}^{pm})(V_i^m - V_k^m)]^* \tag{17}$$

By separating the real and imaginary part of complex branch flow equation (17), we get equations (18) and (19).

$$P_{ik}^p = \sum_{m=1}^{3} \{|V_i^p||V_i^m| cos{\theta_V}_{ii}^{pm} G_{ik}^{pm} - |V_i^p||V_k^m| cos{\theta_V}_{ik}^{pm} G_{ik}^{pm} + |V_i^p||V_i^m| sin{\theta_V}_{ii}^{pm} B_{ik}^{pm} - |V_i^p||V_k^m| sin{\theta_V}_{ik}^{pm} B_{ik}^{pm}\} \tag{18}$$

$$Q_{ik}^p = \sum_{m=1}^{3} \{|V_i^p||V_i^m| sin{\theta_V}_{ii}^{pm} G_{ik}^{pm} - |V_i^p||V_k^m| sin{\theta_V}_{ik}^{pm} G_{ik}^{pm} - |V_i^p||V_i^m| cos{\theta_V}_{ii}^{pm} B_{ik}^{pm} + |V_i^p||V_k^m| cos{\theta_V}_{ik}^{pm} B_{ik}^{pm}\} \tag{19}$$

Equation (18) can be simplified as follows by the assuming $|V_i^p| \approx 1$.

$$P_{ik}^p = \sum_{m=1}^{3} 2B_{ik}^{pm} sin\left(\frac{{\theta_V}_i^p - {\theta_V}_i^m - {\theta_V}_i^p + {\theta_V}_k^m}{2}\right) cos\left(\frac{{\theta_V}_i^p - {\theta_V}_i^m + {\theta_V}_i^p - {\theta_V}_k^m}{2}\right) - \sum_{m=1}^{3} 2G_{ik}^{pm} sin\left(\frac{{\theta_V}_i^p - {\theta_V}_i^m - {\theta_V}_i^p + {\theta_V}_k^m}{2}\right) sin\left(\frac{{\theta_V}_i^p - {\theta_V}_i^m + {\theta_V}_i^p - {\theta_V}_k^m}{2}\right) \tag{20}$$

If we assume balanced voltage angles,

$${\theta_V}_i^p - {\theta_V}_i^m + {\theta_V}_i^p - {\theta_V}_k^m \approx \begin{cases} 240^\circ & \text{if } p-m=-1,2 \\ -240^\circ & \text{if } p-m=1,-2 \\ 0^\circ & \text{if } p-m=0 \end{cases}$$

We have $sin{\theta_V}_{ik}^{mm} \approx {\theta_V}_{ik}^{mm}$. Now equation (20) can be simplified as follows.

$$P_{ik}^p = \sum_{m=1}^{3} \left(B_{P_{ik}}^{pm}\right)'' ({\theta_V}_i^m - {\theta_V}_k^m) \tag{21}$$

where

$$(B_P{}_{ik}^{pm})^{"} = \begin{cases} \frac{1}{2}B_{ik}^{pm} + \frac{\sqrt{3}}{2}G_{ik}^{pm} & \text{if } p-m=-1,2; \\ \frac{1}{2}B_{ik}^{pm} - \frac{\sqrt{3}}{2}G_{ik}^{pm} & \text{if } p-m=1,-2; \\ -B_{ik}^{pm} & \text{if } p-m=0. \end{cases}$$

According to equation (21), the change in real power branch flow ΔP_B can be represented in condensed form as:

$$\Delta P_B = [D_P][A]\Delta\theta_V \tag{22}$$

where ΔP_B is a $3L \times 1$ vector. L is the total number of branches. $[D_P]$ is a $3L \times 3L$ matrix, whose off-diagonal 3×3 blocks are zeros. Let D_{Pb} denote the *b*-th 3×3 diagonal block connecting bus *i* and bus *k*

$$D_{Pb} = \begin{bmatrix} -B_{ik}^{11} & \frac{1}{2}B_{ik}^{12} + \frac{\sqrt{3}}{2}G_{ik}^{12} & \frac{1}{2}B_{ik}^{13} - \frac{\sqrt{3}}{2}G_{ik}^{13} \\ \frac{1}{2}B_{ik}^{21} - \frac{\sqrt{3}}{2}G_{ik}^{21} & -B_{ik}^{22} & \frac{1}{2}B_{ik}^{23} + \frac{\sqrt{3}}{2}G_{ik}^{23} \\ \frac{1}{2}B_{ik}^{31} + \frac{\sqrt{3}}{2}G_{ik}^{31} & \frac{1}{2}B_{ik}^{32} - \frac{\sqrt{3}}{2}G_{ik}^{32} & -B_{ik}^{33} \end{bmatrix}$$

[*A*] is a $3L \times 3(N-1)$ node-arc incidence matrix. [*A*] is compromised of $L \times (N-1)$, 3 by 3 blocks. Each row of the 3×3 blocks represents a three-phase branch. Each column of the 3×3 blocks represents a bus. Let $[A_{ij}]$ be the *ij*-th 3×3 block of [*A*].

$$\text{Diagonals of } A_{ij} = \begin{cases} 1 & \text{if branch } i \text{ starts at node } j \\ -1 & \text{if if branch } i \text{ ends at node } j \\ 0 & \text{otherwise} \end{cases}$$

The non-diagonal elements of $[A_{ij}]$ are zeros.

Substituting equation (11) into (22) yields

$$\begin{aligned} \Delta P_B &= [D_P][A]\Delta\theta_V \\ &= [D_P][A][B_P]^{-1}\Delta P \end{aligned} \tag{23}$$

Therefore, three-phase generation shift factor matrix for real power flow is derived as:

$$[GSFP] = [D_P][A][B_P]^{-1} \tag{24}$$

With $|V_i^p| \approx 1$ and the balanced angle assumption:

$$\theta_V{}_{ii}^{pm} \approx \theta_V{}_{ik}^{pm} = \begin{cases} 120^\circ & \text{if } p-m=-1,2; \\ -120^\circ & \text{if } p-m=1,-2? \\ 0^\circ & \text{if } p-m=0. \end{cases}$$

Equation (19) can be simplified as:

$$Q_{ik}^p = \sum_{m=1}^{3} \left(G_{ik}^{pm} sin\theta_V{}^{pm} - B_{ik}^{pm} cos\theta_V{}^{pm}\right)\left(|V_i^m| - |V_k^m|\right) \tag{25}$$

Therefore

$$Q_{ik}^p = \sum_{m=1}^{3} (B_Q{}_{ik}^{pm})^{''}\left(|V_i^m| - |V_k^m|\right) \tag{26}$$

where

$$(B_Q{}_{ik}^{pm})^{"} = \begin{cases} \frac{1}{2}B_{ik}^{pm} + \frac{\sqrt{3}}{2}G_{ik}^{pm} & \text{if } p-m=-1,2; \\ \frac{1}{2}B_{ik}^{pm} - \frac{\sqrt{3}}{2}G_{ik}^{pm} & \text{if } p-m=1,-2; \\ -B_{ik}^{pm} & \text{if } p-m=0. \end{cases}$$

According to equation (26), the change in reactive power branch flow ΔQ_B can be represented in condensed form as:

$$\Delta Q_B = [D_Q][A]\Delta V \tag{27}$$

where Q_B is a $3L \times 1$ vector. L is the total number of branches. D_Q is a $3L \times 3L$ matrix, whose off-diagonal 3×3 blocks are zeros. Let the D_{Q_b} denote the *b*-th 3×3 diagonal block connecting node *i* and node *k*.

$$D_{Q_b} = \begin{bmatrix} -B_{ik}^{11} & \frac{1}{2}B_{ik}^{12} + \frac{\sqrt{3}}{2}G_{ik}^{12} & \frac{1}{2}B_{ik}^{13} - \frac{\sqrt{3}}{2}G_{ik}^{13} \\ \frac{1}{2}B_{ik}^{21} - \frac{\sqrt{3}}{2}G_{ik}^{21} & -B_{ik}^{22} & \frac{1}{2}B_{ik}^{23} + \frac{\sqrt{3}}{2}G_{ik}^{23} \\ \frac{1}{2}B_{ik}^{31} + \frac{\sqrt{3}}{2}G_{ik}^{31} & \frac{1}{2}B_{ik}^{32} - \frac{\sqrt{3}}{2}G_{ik}^{32} & -B_{ik}^{33} \end{bmatrix}$$

Similarly, with equations (16) and (27), three-phase generation shift factor matrix for reactive power flow is derived as:

$$[GSFQ] = [D_Q][A][B_Q]^{-1} \tag{28}$$

The derivations of three-phase GSFs have the same form as single-phase GSF matrix. However, matrices $[D_P]$, $[D_Q]$, $[A]$, $[B_P]$ and $[B_Q]$ are constructed in a different way. Intuitively, the differences arise from the mutual coupling among three phases of distribution system line. All of the non-diagonal elements of $[D]$ in single-phase GSF equation are zeros, while non-diagonal elements of diagonal 3 by 3 blocks of $[D_P]$ and $[D_Q]$ in three-phase GSF equations are typically non-zero. In three-phase equations $[B_P]$ and $[B_Q]$ are constructed with conductance and susceptance from the admittance matrix Y.

C. Centralized Loss Model

The power loss on each branch can be written as:

$$\begin{aligned} (S_{Loss})_{ik} &= V_{ik} \cdot {I_{ik}}^* = (Z_{ik}I_{ik}) \cdot {I_{ik}}^* \\ &= \left(\begin{bmatrix} Z_{ik}^{11} & Z_{ik}^{12} & Z_{ik}^{13} \\ Z_{ik}^{21} & Z_{ik}^{22} & Z_{ik}^{23} \\ Z_{ik}^{31} & Z_{ik}^{32} & Z_{ik}^{33} \end{bmatrix} I_{ik} \right) \cdot {I_{ik}}^* \end{aligned} \tag{29}$$

For each phase, we have:

$$(S_{Loss})_{ik}^p = {I_{ik}^p}^* \sum_{g=1}^{3} Z_{ik}^{pg} I_{ik}^g \tag{30}$$

where Z_{ik}^{pg} is the element of phase impedance matrix relating node *i* with phase *p* and node *k* with phase *g*. ${I_{ik}^p}^* = |I_{ik}^p| e^{-j\theta_{ik}^p}$ and $I_{ik}^g = |I_{ik}^g| e^{j\theta_{ik}^g}$

Assume $|I_{ik}^g| \approx |I_{ik}^p|, for\, p \neq g$, then (30) can be simplified as:

$$\begin{aligned} (S_{Loss})_{ik}^p &= |I_{ik}^p|^2 \sum_{g=1}^{3} Z_{ik}^{pg} \left(cos\theta_I{}_{ik}^{pg} - j \cdot sin\theta_I{}_{ik}^{pg}\right) \\ &= |I_{ik}^p|^2 \sum_{g=1}^{3} \left(R_{ik}^{pg} + jX_{ik}^{pg}\right)\left(cos\theta_I{}_{ik}^{pg} - j \cdot sin\theta_I{}_{ik}^{pg}\right) \end{aligned} \tag{31}$$

The real part of (31) is the real power loss,

$$(P_{Loss})_{ik}^{p} = \sum_{g=1}^{3} |I_{ik}^{p}|^{2} \left(R_{ik}^{pg} \cos\theta_{I_{ik}^{pg}} + X_{ik}^{pg} \sin\theta_{I_{ik}^{pg}}\right) = \sum_{g=1}^{3} \frac{|S_{ik}^{p}|^{2}}{|V_{i}^{p}|^{2}} R_{ik}^{pg\prime} \quad (32)$$

Where the equivalent resistance obtained from phase impedance matrix relating node *i* with phase *p* and node *k* with phase *g* is defined as: $R_{ik}^{pg\prime} \triangleq R_{ik}^{pg} \cos\theta_{I_{ik}^{pg}} + X_{ik}^{pg} \sin\theta_{I_{ik}^{pg}}$.

If balanced current angle is assumed,

$$\theta_{I_i}^{p} - \theta_{I_k}^{g} = \begin{cases} 120^{\circ} & \text{if } p-g=-1,2 \\ -120^{\circ} & \text{if } p-g=1,-2 \\ 0^{\circ} & \text{if } p-g=0. \end{cases}$$

Then

$$R_{ik}{}' = \begin{bmatrix} R_{ik}^{11} & -\frac{1}{2}R_{ik}^{12} + \frac{\sqrt{3}}{2}X_{ik}^{12} & -\frac{1}{2}R_{ik}^{13} - \frac{\sqrt{3}}{2}X_{ik}^{13} \\ -\frac{1}{2}R_{ik}^{21} - \frac{\sqrt{3}}{2}X_{ik}^{21} & R_{ik}^{22} & -\frac{1}{2}R_{ik}^{23} + \frac{\sqrt{3}}{2}X_{ik}^{23} \\ -\frac{1}{2}R_{ik}^{31} + \frac{\sqrt{3}}{2}X_{ik}^{31} & -\frac{1}{2}R_{ik}^{32} - \frac{\sqrt{3}}{2}X_{ik}^{32} & R_{ik}^{33} \end{bmatrix}_{ik}$$

If we assume $|V_i^p| \approx 1$, then (32) can be simplified as:

$$(P_{Loss})_{ik}^{p} = \sum_{g=1}^{3} |S_{ik}^{p}|^{2} R_{ik}^{pg\prime} = \sum_{g=1}^{3} (|P_{ik}^{p}|^{2} + |Q_{ik}^{p}|^{2}) R_{ik}^{pg\prime} \quad (33)$$

Therefore we have

$$P_{Loss}^{p} = P_{Loss}^{p}(FP) + P_{Loss}^{p}(FQ) \quad (34)$$

where

$$P_{Loss}^{p}(FP) = \sum_{b=1}^{B}\sum_{g=1}^{3} \left(FP_{b}^{p}\right)^{2} R_{b}^{pg\prime}$$

$$P_{Loss}^{p}(FQ) = \sum_{b=1}^{B}\sum_{g=1}^{3} \left(FQ_{b}^{p}\right)^{2} R_{b}^{pg\prime}$$

where B is the total number of branches. FP_b^p and FQ_b^p are real and reactive power flow on branch b at phase g. FP and FQ are the set of real and reactive branch flows respectively. F_b^p can be obtained with GSFs and power injections:

$$FP_{b}^{p} = \sum_{q=2}^{N}\sum_{m=1}^{3} GSF_{b\_q}^{p\_m} P_{q}^{m} \quad (35)$$

$$FQ_{b}^{p} = \sum_{q=2}^{N}\sum_{m=1}^{3} GSF_{b\_q}^{p\_m} Q_{q}^{m} \quad (36)$$

Phase *p*'s marginal loss factor (LF) at bus *s* with phase *t* is defined as follows:

$$(LF_{s}^{t})^{p} \triangleq \frac{\partial P_{Loss}^{p}}{\partial P_{s}^{t}} = \sum_{b=1}^{B}\sum_{g=1}^{3} 2R_{b}^{pg\prime} \cdot GSFP_{b\_s}^{p\_t} \sum_{q=2}^{N}\sum_{m=1}^{3} GSFP_{b\_q}^{p\_m} P_{q}^{m} \quad (37)$$

Phase *p*'s marginal delivery factor (DF) at bus *s* with phase *t* is defined as following:

$$(DF_{s}^{t})^{p} \triangleq \begin{cases} 1-(LF_{s}^{t})^{p}, t=p, \\ -(LF_{s}^{t})^{p}, t\neq p \end{cases} \quad (38)$$

Loss factor and delivery factor are keys to deriving marginal loss component of LMP. The definitions of three-phase LF and DF are similar to that of single-phase. However, from Equation (38), we can clearly see that in three-phase distribution systems, power losses of one phase is influenced by net loads of the other phases. Delivery factor $(DF_s^t)^p$ is the amount of power delivered from phase *p* when the load on node *s* with phase *t* increases by 1KW. When *t* equals *p*, DF is the sum of increase of load and power losses due to real power flow on phase *p*. Otherwise, DF is equal to the increase in power losses due to real power flow on phase *p*.

With the definitions above, it can be proved that

$$\begin{aligned} &\sum_{s=1}^{N}\sum_{t=1}^{3} (DF_{s}^{t})^{p} \cdot \left(PG_{s}^{t} - PD_{s}^{t}\right) = \sum_{s=1}^{N}\sum_{t=1}^{3} (DF_{s}^{t})^{p} P_{s}^{t} \\ &= \sum_{s=1}^{N} P_{s}^{p} - \sum_{s=1}^{N}\sum_{t=1}^{3} \left[\left(\sum_{b=1}^{B}\sum_{g=1}^{3} 2 \cdot R_{b}^{pg\prime} GSFP_{b\_s}^{p\_t} FP_{b}^{p}\right) \cdot P_{s}^{t}\right] \\ &= \sum_{s=1}^{N} P_{s}^{p} - \sum_{b=1}^{B}\sum_{g=1}^{3} \left(2 \cdot R_{b}^{pg\prime} FP_{b}^{p} \sum_{s=1}^{N}\sum_{t=1}^{3} GSFP_{b\_s}^{p\_t} P_{s}^{t}\right) \\ &= \sum_{s=1}^{N} P_{s}^{p} - 2\sum_{b=1}^{B}\sum_{g=1}^{3} R_{b}^{pg\prime} \left(FP_{b}^{p}\right)^{2} \\ &= -P_{Loss}^{p}(FP) + P_{Loss}^{p}(FQ) \end{aligned} \quad (39)$$

Thus the real power balance constraints become:

$$\sum_{i=1}^{N}\sum_{m=1}^{3} (DF_{i}^{m})^{p} \cdot PG_{i}^{m} - \sum_{i=1}^{N}\sum_{m=1}^{3} (DF_{i}^{m})^{p} \cdot PD_{i}^{m} + P_{Loss}^{p}(FP) - P_{Loss}^{p}(FQ) = 0, p = 1,2,3 \quad (40)$$

D. FND Model

Adopting FND can distribute system losses among distribution lines to eliminate significant mismatch at the reference bus. FND-based DCOPF yields a closer approximation to the results of ACOPF, as shown in [19]. E_i^p, FND at bus *i* with phase *p*, is defined as following:

$$E_{i}^{p} = \frac{1}{2}\sum_{b=1}^{B_i}\sum_{g=1}^{3} [\left(FP_{b}^{g}\right)^{2} + \left(FQ_{b}^{g}\right)^{2}] R_{b}^{pg\prime} \quad (41)$$

where B_i is the number of branches connected to bus *i*. With FND, the power injection at each node becomes:

$$P_{q}^{m} = PG_{q}^{m} - PD_{q}^{m} - E_{q}^{m} \quad (42)$$

Using FND, branch flow equation (35) can be updated as:

$$FP_{b}^{g} = \sum_{q=2}^{N}\sum_{m=1}^{3} GSFP_{b\_q}^{g\_m} \left(PG_{q}^{m} - PD_{q}^{m} - E_{q}^{m}\right) \quad (43)$$

$$\psi=\left(\sum_{n=1}^{N}\sum_{m=1}^{3}\left(\sum_{j=1}^{J_n^m}Cd\left(n,m\right)_j d\left(n,m\right)_j-\sum_{i=1}^{I_n^m}Cg\left(n,m\right)_i g\left(n,m\right)_i\right)\right)-\sum_{p=1}^{3}\lambda^p\left(\sum_{i=1}^{N}\sum_{m=1}^{3}(DF_i^m)^p\cdot PG_i^m\right.$$
$$\left.-\sum_{i=1}^{N}\sum_{m=1}^{3}(DF_i^m)^p\cdot(PD_i^m+E_i^m)+P_{Loss}^p(FP)-P_{Loss}^p(FQ)\right)-\sum_{b=1}^{B}\sum_{p=1}^{3}\mu_b^{p+}\left(\sum_{q=1}^{N}\sum_{g=1}^{3}GSFP_{b\_q}^{p\_g}\cdot P_q^g-PLimit_b^p\right)$$
$$-\sum_{b=1}^{B}\sum_{p=1}^{3}\mu_b^{p-}\left(-\sum_{q=1}^{N}\sum_{g=1}^{3}GSFP_{b\_q}^{p\_g}\cdot P_q^g-PLimit_b^p\right)-\sum_{p=1}^{2}\sum_{m=2,m\neq p}^{3}\mu^{pm+}\left(\sum_{n=2}^{N}P_n^p-\sum_{n=2}^{N}P_n^m-\gamma\right)$$
$$-\sum_{p=1}^{2}\sum_{m=2,m\neq p}^{3}\mu^{pm-}\left(-\sum_{n=2}^{N}P_n^p+\sum_{n=2}^{N}P_n^m-\gamma\right) \quad (45)$$

Thus, power flow constraints (3) are revised as:

$$|\sum_{q=2}^{N}\sum_{g=1}^{3}GSFP_{ik\_q}^{p\_g}\cdot\left(PG_q^g-PD_q^g-E_q^m\right)|^2\leq PLimit_{ik}^p,$$
$$\forall i,k \quad and \quad i\neq k \quad (44)$$

Then the values of LFs, DFs, and power losses are updated with the new power injections and power flows calculated from equations (42)-(43).

E. Iterative DCOPF Algorithm

The FND-based DCOPF problem is solved iteratively. The iterative algorithm we propose can be briefly described as follows:

1) Initially set LFs, FNDs and power losses to zeros.
2) Solve linear optimization problem using (1), (4), (40), and (44).
3) Update the values of FNDs, power losses, LFs and DFs using (37), (38), (41) and (43).
4) Solve the linear optimization problem again using (1), (4), (40), and (44).
5) Check the dispatch of loads and generation resources. If the difference between the current iteration and previous iteration's result is larger than the pre-defined tolerance, go the step 3. Otherwise, the final three-phase OPF solution is obtained.

III. Three-Phase LMP Decomposition

LMP at node *i* with phase *g* can be derived by differentiating Lagrangian function (45) with respect to fixed load at node *i* phase *g*. Lagrangian function ψ is derived from objective function (1) and constraints (4), (40), and (44). λ^p is the Lagrange multiplier of real power balance constraint of phase *p* (40); μ_b^{p+} and μ_b^{p-} are the Lagrange multipliers of distribution line thermal limit constraints (44); μ^{pm+} and μ^{pm-} are the Lagrange multipliers of phase imbalance constraints (4).

As shown in (46), three-phase LMPs can be decomposed into four component: marginal energy component, marginal loss component, marginal congestion component, and marginal phase imbalance component. Compared with single-phase LMP, three-phase LMP has an extra component, namely, marginal phase imbalance component.

$$LMP_i^g=\frac{\partial\psi}{\partial FD_i^g}$$
$$=\sum_{p=1}^{3}\lambda^p(DF_i^g)^p+\sum_{b=1}^{B}\sum_{p=1}^{3}\mu_b^{p\prime}GSFP_{b\_i}^{p\_g}+\mu^{g\prime\prime}$$
$$=\lambda^g-\sum_{p=1}^{3}\lambda^p(LF_i^g)^p+\sum_{b=1}^{B}\sum_{p=1}^{3}\mu_b^{p\prime}GSFP_{b\_i}^{p\_g}+\mu^{g\prime\prime} \quad (46)$$

where

$$\mu_b^{p\prime}=\mu_b^{p+}-\mu_b^{p-}$$
$$\mu^{g\prime\prime}=\begin{cases}\mu^{12+}+\mu^{13}-\mu_i^{12-}-\mu^{13-} & \text{if } g=1;\\ -\mu^{12+}+\mu^{23}+\mu_i^{12-}-\mu^{23-} & \text{if } g=2;\\ -\mu^{13+}-\mu^{23}+\mu_i^{13-}+\mu^{23-} & \text{if } g=3.\end{cases}$$

IV. Numerical Study

In this section, a benchmark three-phase ACOPF algorithm is first briefly presented. The proposed three-phase DCOPF algorithm is then compared with the ACOPF algorithm using the IEEE 4-bus test system. At last, the decomposition of the three-phase LMPs is illustrated with the test system.

A. Three-phase ACOPF Algorithm

The benchmark ACOPF algorithm is based on an extension of the SDP algorithm [10] to three-phase system with rank reduction technique described in [18]. The optimality of ACOPF algorithm can be validated with the conditions stated in [10] for the convex iteration algorithm. Note that this ACOPF algorithm cannot be easily scaled up due to the curse of dimensionality.

B. Simulation Setup

The simulation is based on the modified IEEE 4-bus test case. The quantity of fixed demand and price sensitive demand of node 4 are shown in Table I. The demand bid curves of flexible loads on three-phases are modeled as step functions shown in Figure 1. The 10 steps of each demand bid curve are assumed to have equal length. The price ranges of the

three price sensitive demand bid curves are from \$0.1/kWh to \$1/kWh. To study the impact of bus voltage deviation on the accuracy of the proposed DCOPF algorithm, simulations are conducted by increasing the reference bus voltage from 1.0 to 1.15 per unit with a step size of 0.01. The base phase-to-neutral voltage of the distribution network is 7.2 KV.

TABLE I
LOAD PROFILE ON NODE 4

Node 4	Phase A	Phase B	Phase C	Total
Fixed Load Capacity (KW)	500	500	500	1500
Flexible Load Capacity (KW)	250	300	350	900

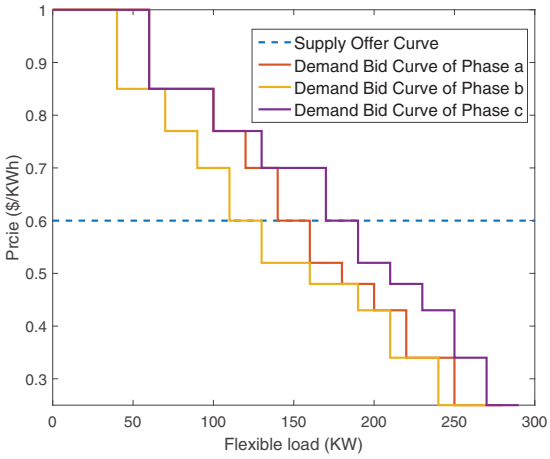

Fig. 1. Demand bid curve of flexible load

C. Simulation Results

1) A comparison between three-phase DCOPF and three-phase ACOPF: The simulation results of three-phase DCOPF and three-phase ACOPF are shown in Table II when the voltage of the reference bus is at 1.0 per unit. As shown in Table II, the differences in social welfare, system real power losses, and real power line flows are very small between the proposed three-phase DCOPF and the benchmark three-phase ACOPF algorithm. The differences in reactive power flow are slightly larger than the real power flow due to the fact that reactive power losses are not modeled in the three-phase DCOPF algorithm. However, as the power factors of distribution loads are typically around 0.95 lagging, the errors of reactive power flow are usually not very significant.

Numerical errors of real power losses and total social welfare are calculated for the proposed three-phase DCOPF algorithm. Figure 2. depicts the change in the numerical errors with various load bus voltage levels. The proposed three-phase DCOPF algorithm achieves best accuracy when the load bus three-phase average voltage is around 1.05 per unit. If the load bus voltage is kept between 0.98 and 1.02 per unit, then the errors of social welfare and real power losses associate with

TABLE II
COMPARISON BETWEEN THREE-PHASE DCOPF AND THREE-PHASE ACOPF

	DCOPF	ACOPF
Social Welfare (\$)	833.4	838.6
Real Power Loss (KW)	38.9	47.1
Power Flows: Line 1 (KVA)	613+242.2i 631.4+242.2i 654.6+242.2i	618.6+281.6i 633.6+281.5i 654.9+288.7i
Power Flows: Line 2 (KVA)	611.5+242.2i 629.9+242.i 652.8+242.2i	617.2 + 279.5i 632.7+279.5i 653.9+286.2i
Power Flows: Line 3 (KVA)	605.2+242.i 624.4+242.2i 645.7+242.2i	614.9+265.7i 630.3+265.1i 651.3+270.8i

the three-phase DCOPF algorithm are smaller than 0.5% and 10% respectively.

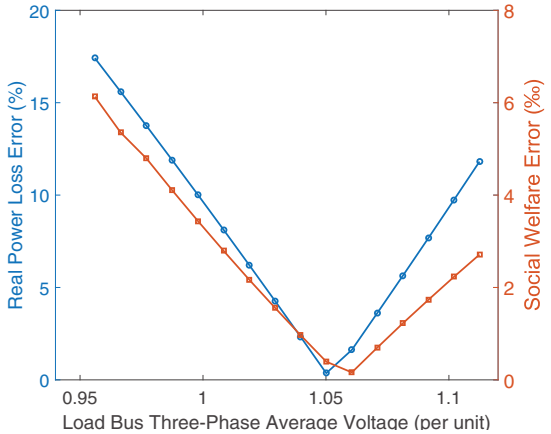

Fig. 2. Numerical error versus load bus voltage

2) Three-phase LMP decomposition: The LMPs of the IEEE 4-bus network are shown in Table III. As illustrated in equation (46), three-phase LMPs consists of marginal energy component, marginal loss component, marginal congestion component, and marginal phase imbalance component. However, because the congestion constraints and phase imbalance constraints are not binding, these two components are not present in Table III. The marginal energy components are \$0.6/kWh for every single bus and phase in the network. The marginal loss components and loss factors increase from distribution substation to the end of the feeder. The marginal loss components are higher on phase c whose loads are slightly higher than that of phase a and b. In order to show the effects of marginal phase imbalance component, simulations are performed by setting the fixed load of phase a as 460 KW and the fixed load of phase c as 530KW. The phase imbalance limit is set as 50 KW. The result of LMPs is shown in Table

IV. The phase imbalance constraint relating phase *a* and *c* is binding. The marginal imbalance price component of phase *a* is about \$-0.1/kWh, while the marginal imbalance price component of phase *c* is about \$0.1/kWh. Phase imbalance components of three-phase LMPs are crucial economic signals sent to customers on phase *a* and *c* instructing them to adjust load level to alleviate phase imbalance problems. The effect of congestion component is intuitive and straightforward.

TABLE III
THREE-PHASE LMPS WITH ONLY ENERGY AND LOSS COMPONENTS

Price (\$/KWh)	Node 2	Node 3	Node 4
Phase A	$0.6 + 0.0016$	$0.6 + 0.0053$	$0.6 + 0.0234$
Phase B	$0.6 + 0.0013$	$0.6 + 0.0051$	$0.6 + 0.02$
Phase C	$0.6 + 0.0016$	$0.6 + 0.0055$	$0.6 + 0.0228$

TABLE IV
THREE-PHASE LMPS WITH ENERGY, LOSS, AND PHASE IMBALANCE COMPONENTS

		Price (\$/KWh)
Node2	Phase A	$0.6 + 0.0016 - 0.1033$
	Phase B	$0.6 + 0.0052 - 0.1033$
	Phase C	$0.6 + 0.0228 - 0.1033$
Node3	Phase A	$0.6 + 0.0013 + 0$
	Phase B	$0.6 + 0.0051 + 0$
	Phase C	$0.6 + 0.0200 + 0$
Node4	Phase A	$0.6 + 0.0015 + 0.1033$
	Phase B	$0.6 + 0.0054 + 0.1033$
	Phase C	$0.6 + 0.0226 + 0.1033$

V. CONCLUSION

This paper develops a three-phase iterative DCOPF algorithm with fictitious nodal demand. GSF matrix, LF, and DF are derived within the three-phase DCOPF framework. The derivation for three-phase LMP decomposition shows that LMP can be decomposed into four price components: marginal energy component, marginal loss component, marginal congestion component, and marginal phase imbalance component. Simulation results from the IEEE 4-bus test case demonstrated the validity of the proposed three-phase DCOPF algorithm. The three-phase DCOPF algorithm is shown to be a good approximation of the ACOPF algorithm when the load bus voltage is within normal operating range.

ACKNOWLEDGMENT

The authors would like to thank Robert Sherick, Araya Gebeyehu, and Stephen Collins from Southern California Edison (SCE) for their helpful discussions and reviews. This work was supported by National Science Foundation (NSF) under award #1637258, California Energy Commission (CEC) under agreement EPC-15-090 and grant from SCE.

REFERENCES

[1] P. M. Sotkiewicz and J. M. Vignolo, "Nodal pricing for distribution networks: efficient pricing for efficiency enhancing DG," *IEEE Trans. Power Syst.*, vol. 21, no. 2, pp. 1013–1014, May 2006.

[2] A. J. Conejo, J. M. Morales, and L. Baringo, "Real-time demand response model," *IEEE Trans. Smart Grid*, vol. 1, no. 3, pp. 236–242, Dec. 2010.

[3] B. Moradzadeh and K. Tomsovic, "Two-stage residential energy management considering network operational constraints," *IEEE Trans. Smart Grid*, vol. 4, no. 4, pp. 2339–2346, Dec. 2013.

[4] N. Yu, T. Wei, and Q. Zhu, "From passive demand response to proactive demand participation," in *2015 IEEE International Conference on Automation Science and Engineering (CASE)*, Aug. 2015, pp. 1300–1306.

[5] T. Wei, Q. Zhu, and N. Yu, "Proactive demand participation of smart buildings in smart grid," *IEEE Trans. Comput.*, vol. 65, no. 5, pp. 1392–1406, May 2016.

[6] M. Hong, X. Yu, N. P. Yu, and K. A. Loparo, "An energy scheduling algorithm supporting power quality management in commercial building microgrids," *IEEE Trans. Smart Grid*, vol. 7, no. 2, pp. 1044–1056, Mar. 2016.

[7] S. Bruno, S. Lamonaca, G. Rotondo, U. Stecchi, and M. L. Scala, "Unbalanced three-phase optimal power flow for smart grids," *IEEE Trans. Ind. Electron.*, vol. 58, no. 10, pp. 4504–4513, Oct. 2011.

[8] E. Dall'Anese, H. Zhu, and G. B. Giannakis, "Distributed optimal power flow for smart microgrids," *IEEE Trans. Smart Grid*, vol. 4, no. 3, pp. 1464–1475, Sept. 2013.

[9] B. H. Kim and R. Baldick, "A comparison of distributed optimal power flow algorithms," *IEEE Trans. Power Syst.*, vol. 15, no. 2, pp. 599–604, May 2000.

[10] J. Lavaei and S. H. Low, "Zero duality gap in optimal power flow problem," *IEEE Trans. Power Syst.*, vol. 27, no. 1, pp. 92–107, Feb. 2012.

[11] Z. q. Luo, W. k. Ma, A. M. c. So, Y. Ye, and S. Zhang, "Semidefinite relaxation of quadratic optimization problems," *IEEE Signal. Proc. Mag.*, vol. 27, no. 3, pp. 20–34, May 2010.

[12] D. K. Molzahn, J. T. Holzer, B. C. Lesieutre, and C. L. DeMarco, "Implementation of a large-scale optimal power flow solver based on semidefinite programming," *IEEE Transactions on Power Systems*, vol. 28, no. 4, pp. 3987–3998, Nov. 2013.

[13] X. Bai, H.Wei, K. Fujisawa, and Y. Wang, "Semidefinite programming for optimal power flow problems," *International Journal of Electric Power and Energy Systems*, vol. 30, no. 6, pp. 383–392, Sept. 2008.

[14] J. Lavaei, D. Tse, and B. Zhang, "Geometry of power flows in tree networks," in *2012 IEEE Power and Energy Society General Meeting*, July 2012, pp. 1–8.

[15] L. Gan, N. Li, U. Topcu, and S. H. Low, "Exact convex relaxation of optimal power flow in radial networks," *IEEE Transactions on Automatic Control*, vol. 60, no. 1, pp. 72–87, Jan. 2015.

[16] S. You and Q. Peng, "A non-convex alternating direction method of multipliers heuristic for optimal power flow," in *Smart Grid Communications (SmartGridComm), 2014 IEEE International Conference on*, Nov. 2014, pp. 788–793.

[17] D. K. Molzahn, C. Josz, I. A. Hiskens, and P. Panciatici, "A Laplacian-based approach for finding near globally optimal solutions to opf problems," *IEEE Trans. Power Syst.*, no. 99, pp. 1–1, 2016.

[18] J. Dattorro, *Convex optimization and Euclidean distance geometry*. CA: Meboo, 2005.

[19] F. Li and R. Bo, "DCOPF-based LMP simulation: Algorithm, comparison with ACOPF, and sensitivity," *IEEE Trans. Power Syst.*, vol. 22, no. 4, pp. 1475–1485, Nov. 2007.

[20] J. Arrillaga and B. J. Harker, "Fast-decoupled three-phase load flow," *Electrical Engineers, Proceedings of the Institution of*, vol. 125, no. 8, pp. 734–740, Aug. 1978.